Accounting for Tomographic Resolution in Estimating Hydrologic Properties from Geophysical Data

Kamini Singha

Department of Geosciences, The Pennsylvania State University, University Park, Pennsylvania, USA

Frederick D. Day-Lewis

U.S. Geological Survey, Office of Ground Water, Branch of Geophysics, Storrs, Connecticut, USA

Stephen Moysey

School of the Environment, Clemson University, Clemson, South Carolina, USA

Geophysical measurements increasingly are being used in hydrologic field studies because of their ability to provide high-resolution images of the subsurface. In particular, tomographic imaging methods can produce maps of physical property distributions that have significant potential to improve subsurface characterization and enhance monitoring of hydrologic processes. In the tomographic imaging approach, geophysical images of the subsurface are converted to hydrologic property maps using petrophysical relations. In field studies, this transformation is complicated because measurement sensitivity and averaging during data inversion result in tomographic images that have spatially variable resolution (i.e., the estimated property values in the geophysical image represent averages of the true subsurface properties). Standard approaches to petrophysics do not account for variable geophysical resolution, and thus it is difficult to obtain quantitative estimates of hydrologic properties. We compare two new approaches that account for variable geophysical resolution: a Random Field Averaging (RFA) method and Full Inverse Statistical Calibration (FISt). The RFA approach uses a semi-analytical method whereas FISt calibration is based on a numerical solution to the problem.

1. INTRODUCTION

Data limitations represent the principal impediment to characterize and monitor subsurface hydrologic properties and processes at the field scale. Conventional hydrologic measurements (e.g., aquifer tests or fluid samples) commonly depend on direct access to the subsurface, making them expensive and sparse. Moreover, such measurements either sample conditions local to boreholes or integrate over large volumes of the subsurface. As a result, these measurements carry limited information about aquifer conditions between sampling locations or provide complex averages of properties, making it difficult to assess the distribution of heterogeneity throughout an aquifer. With recent advances in geophysical instrumentation and imaging algorithms, hydrologists increasingly are looking to geophysical imaging methods to help understand aquifer heterogeneity and monitor such processes as contaminant transport and seasonal dynamics in water content.

Title
Geophysical Monograph Series

##.####/###GM##

In recent years, the term "hydrogeophysics" has come to describe these kinds of interdisciplinary research efforts that bridge hydrology and geophysics. This new field is burgeoning, as evidenced by rapid growth of hydrogeophysics papers in the literature, as well as publication of recent texts on the subject [*Rubin and Hubbard*, 2005; *Vereecken et al.*, 2006]. In numerous studies, geophysical imaging has provided valuable data at spatial and temporal scales rarely attainable with standard hydrologic measurements. A conclusion common to much of this work is that the quantitative integration of geophysical and hydrologic data—through either coupled inversion or geostatistical techniques—results in characterization of the subsurface with higher resolution and greater reliability than is possible using conventional hydrologic measurements alone. Despite growing acceptance and clear evidence for the synergies that result from hydrogeophysical data integration, important research challenges remain. One of the foremost problems is determining how geophysical properties determined by a field survey (e.g., electrical conductivity, dielectric permittivity, or seismic velocity) are related to the properties that hydrologists are interested in, such as hydraulic conductivity, contaminant concentration, or water quantity. Petrophysical formulas that describe the relations between these properties are commonly used, and can be calibrated as site-specific conversions [e.g., *Alumbaugh et al.*, 2002] or based on theoretical or general empirical grounds [e.g., *Slater et al.*, 2002; *Singha and Gorelick*, 2005]. Petrophysical relations have been used extensively to convert geophysical images into two-dimensional (2D) maps or three-dimensional (3D) volumes of quantities such as saturation, concentration, porosity, or permeability [e.g., *Hubbard et al.*, 2001; *Slater et al.*, 2002; *Berthold and Masaki*, 2004].

One difficulty with using standard petrophysical relations to convert geophysical to hydrologic property values in tomographic studies is that the data or theory used to generate the relations may not fully capture conditions at the field scale. For example, a petrophysical relation may be based on data from a set of wells or cores. Because of subsurface heterogeneity, these data may be representative of only a small area near where they were collected; consequently, the calibrated petrophysical relation is most certain near the location where the data were collected, and reflects the particular support volume of the measurements at this location. Away from the sampling location, both the resolution of the geophysical survey and the type of material may change, causing the calibrated petrophysical relation to no longer apply. Additionally, the sensitivity of the geophysical methods and the effects of image reconstruction can contribute to the field-scale estimate of a geophysical property, thereby creating spatial dependence in the petrophysical relation. Consequently, relations between, for example, seismic velocity and hydraulic conductivity found at the laboratory scale may not be appropriate in the field. Direct estimation of hydrologic properties from geophysical tomograms at the field scale has been only moderately successful because 1) reconstructed tomograms are often highly uncertain and subject to inversion artifacts; 2) the range of subsurface conditions represented in calibration data sets is incomplete due heterogeneity and the paucity of collocated well or core data; and 3) geophysical methods exhibit spatially variable sensitivity.

The uncertainty and non-uniqueness of petrophysical relations have led some to consider stochastic methods, such as co-simulation and co-kriging frameworks [e.g., *McKenna and Poeter*, 1995; *Cassiani et al.*, 1998; *Yeh et al.*, 2002; *Ramirez et al.*, 2005] or other geostatistical approaches for incorporating geophysical property estimates into hydrogeologic studies, such as the 1) correlation of site-specific soft geophysical data with collocated hard point data [*Doyen*, 1988; *McKenna and Poeter*, 1995; *Dietrich et al.*, 1998], 2) estimation of hydrologic properties from geophysical data based on probabilities of occurrence as mapped by geologists [*Carle and Ramirez*, 1999], and 3) estimation using geophysical methods for lithologic zonation [*Hyndman et al.*, 1994; *Hyndman and Gorelick*, 1996]. Some approaches to data integration include coupled inversion methods that consider hydrologic processes directly. For example, *Vanderborght et al.* [2005] used equivalent advection-dispersion equations and streamtube models to quantify breakthrough curves from synthetic 2D electrical resistivity tomography (ERT) inversions for estimating hydraulic conductivity and local-scale dispersivity values. *Kowalsky et al.* [2005] demonstrated coupled inversion of ground-penetrating radar (GPR) tomographic data and neutron probe data to monitor infiltration processes. Coupled inversion approaches may, in some cases, address the resolution issues related to geophysical imaging by directly integrating geophysical data in the hydrologic estimation problem to identify properties governing flow and transport. While the inherent limitations of geophysical method resolution cannot be fully circumvented, abandoning the idea of producing first a geophysical image may help in that the additional assumptions needed for this purpose (e.g., smoothness) are not necessary, and therefore do not "contaminate" the data inversion.

In this chapter, we work with inverted geophysical images, and highlight previous work regarding the estimation of petrophysical relations and the impacts of tomographic resolution for quantitatively integrating geophysical data into hydrogeologic estimation problems. By comparing emerging petrophysical methods that directly address geophysical resolution, we will offer suggestions for how to address these problems.

2. BACKGROUND

2.1. Traditional Petrophysical Approaches

Theoretical or empirical results are commonly used to develop petrophysical relations. For example, in theoretical studies, effective medium theory is typically used to predict the effective properties of a heterogeneous medium from the properties of its components. A well-known example of this approach to petrophysics was developed by *Hashin and Shtrikman* [1962; 1963] who estimated bounds on the effective magnetic and elastic properties of a composite medium based on the properties of the individual components. Other methods, such as differential effective medium approaches, have been developed when inclusions are sparse and do not form a connected network [e.g., *Berge et al.*, 1993].

At the field scale, interpretation of geophysical data in terms of hydrogeologic properties is often based on the linear regression of field data [e.g., *Kelly*, 1977; *Klimentos and McCann*, 1990; *Purvance and Andricevic*, 2000], or on theoretical relations [e.g., *Urish*, 1981; *Jorgensen*, 1988; *Blair and Berryman*, 1992; *Rubin et al.*, 1992; *Hubbard et al.*, 1997; *Gal et al.*, 1998; *Chan and Knight*, 1999; *Dunn et al.*, 1999; *Wang and Horne*, 2000]. Petrophysical relations can also be determined empirically at the laboratory scale. Two empirical petrophysical relations common in hydrogeophysics are 1) the Topp equation [*Topp et al.*, 1980], where laboratory measurements made on soils were used to fit a polynomial relation between the dielectric constant and water content of a soil, and 2) Archie's law [*Archie*, 1942], where well-log data were used to determine a relation between bulk electrical conductivity and porosity. Research has gone into applying theory to validate these relations, as can be seen in the work of *Hunt* [2004]. *Knight and Endres* [2005] give a comprehensive introduction to traditional petrophysical approaches relevant to hydrogeophysical studies.

Recent work has indicated that laboratory-scale petrophysical relations may not hold at the field scale. *Moysey and Knight* [2004] investigated the relation between dielectric constant and water content assuming that these properties could be represented by spatially correlated random fields. They found that when an electromagnetic wave produced by GPR averages over small-scale heterogeneities, the petrophysical relation at the measurement scale will be different from that defined at the scale of the property variations. Thus, they suggest that a petrophysical relation will be independent of measurement scale only when a medium is self-similar, given the same boundary conditions between the laboratory and field. Studies of this nature demonstrate that understanding how the subsurface is sampled is a critical aspect of developing appropriate petrophysical relations for field-scale problems.

2.2. Inversion and the "Geophysical Filter"

Each geophysical property value estimated in a field survey, such as a tomographic imaging experiment, represents an average of the true properties of the subsurface. Limitations in geophysical resolution mean that this average is rarely representative of only the region of the subsurface contained within the volume defined by a single voxel in the inverted model, leading to the smearing effect that is characteristic of geophysical images. Attempts at quantifying the resolution of the geophysical estimates date to *Backus and Gilbert* [1968], who consider each estimated parameter (or voxel) to depend upon some surrounding model space. Since this seminal work, quantifying tomographic resolution and geophysical measurement support has become an active area of geophysical research [e.g., *Menke*, 1984; *Ramirez et al.*, 1993; *Rector and Washbourne*, 1994; *Schuster*, 1996; *Oldenburg and Li*, 1999; *Alumbaugh and Newman*, 2000; *Friedel*, 2003; *Sheng and Schuster*, 2003; *Dahlen*, 2004]. Resolution has been found to be dependent on the measurement physics; survey design; measurement error; regularization criteria and inversion approach. In other words, the resolution of a target in the subsurface depends not only on the data collection, but on how the data are modeled and inverted. We conceptually refer to the cumulative effect of the factors that cause a loss in resolution between the true distribution of properties in the earth and that estimated by a geophysical survey as the *geophysical filter*.

We use an Occam's inversion, which is closely related to the Gauss-Newton approach (varying only in the explicit way in the which alpha is determined), for geophysical data inversion. We seek to identify the vector of model parameters that minimize an objective function, F, which consists of: 1) the least-squares, weighted misfit between observed and predicted measurements in the first term, and 2) a measure of solution complexity in the second term:

$$F = \left(\mathbf{d} - g\left(\hat{\mathbf{m}}\right)\right)^T \mathbf{C}_D^{-1} \left(\mathbf{d} - g\left(\hat{\mathbf{m}}\right)\right) + \alpha \left(\hat{\mathbf{m}} - \mathbf{m}_0\right)^T \mathbf{D}^T \mathbf{D} \left(\hat{\mathbf{m}} - \mathbf{m}_0\right) \quad (1)$$

where

- $\mathbf{d}$ is the vector of measurements;
- $g(\cdot)$ is the forward model;
- $\hat{\mathbf{m}}$ is the vector of parameter estimates, i.e., the calculated data;
- $\mathbf{m}_0$ is the model prior;
- $\mathbf{C}_D$ is the covariance matrix of measurement errors;
- α is a weight that determines the tradeoff between data misfit and regularization; and
- $\mathbf{D}$ is the model-weighting regularization matrix (e.g., a discretized second-derivative filter).

The model parameters are updated in an iterative fashion by repeated solution of a linear system of equations for $\Delta\hat{\mathbf{m}}$, the model update, at successive iterations such that

$$\left[\mathbf{J}^T\mathbf{C}_D^{-1}\mathbf{J} + \alpha\mathbf{D}^T\mathbf{D}\right]\Delta\hat{\mathbf{m}} = \mathbf{J}^T\mathbf{C}_D^{-1}\left(\mathbf{d} - g\left(\hat{\mathbf{m}}_{k-1}\right)\right) - \alpha\mathbf{D}^T\mathbf{D}\left(\hat{\mathbf{m}}_{k-1} - \mathbf{m}_{prior}\right) \quad (2)$$

$$\hat{\mathbf{m}}_k = \hat{\mathbf{m}}_{k-1} + \Delta\hat{\mathbf{m}} \quad (3)$$

where

$\mathbf{J}$ is the Jacobian matrix, with elements $J_{ij} = \partial\hat{d}_i / \partial\hat{m}_j$;

$\hat{d}_i$ is the calculated value of measurement i;

$\hat{\mathbf{m}}_k$ is the vector of parameter estimates after updating in iteration k; and

$\Delta\hat{\mathbf{m}}$ is the vector of parameter updates for iteration k.

At each iteration of the inversion, a new Jacobian is calculated. A line search is performed to identify the α value such that the new model estimate from solution of equation (2) results in the expected root-mean squared (RMS) prediction error given the model of measurement errors. If such a value cannot be found, then the α that gives the lowest RMS error is taken, and the algorithm proceeds to the next iteration. The inversion continues until 1) the RMS error reaches the target RMS error, 2) the reduction in RMS error between successive iterations or the size of the objective function is less than a specified tolerance, or 3) a maximum number of iterations is reached. This approach is commonly referred to as an Occam inversion.

The model resolution matrix, which describes the degree to which model parameters can be determined independently from each other, can be calculated using the Jacobian matrix. The rows of the resolution matrix should sum to 1, and describe the smearing of the true model parameter; conceptually, the model resolution matrix is the lens or filter through which the inversion sees the study region:

$$\hat{\mathbf{m}} = \left[\mathbf{J}^T\mathbf{C}_D^{-1}\mathbf{J} + \alpha\mathbf{D}^T\mathbf{D}\right]^{-1}\mathbf{J}^T\mathbf{C}_D^{-1}\left(\mathbf{d} - \mathbf{J}\,\mathbf{m}_{prior}\right) + \mathbf{m}_{prior} \approx \left[\mathbf{J}^T\mathbf{C}_D^{-1}\mathbf{J} + \alpha\mathbf{D}^T\mathbf{D}\right]^{-1}\mathbf{J}^T\mathbf{C}_D^{-1}\mathbf{J}\left(\mathbf{m}_{true} - \mathbf{m}_{prior}\right) + \mathbf{m}_{prior}, \quad (4)$$

where the model resolution matrix, $\mathbf{R}$, is defined as

$$\mathbf{R} = \left[\mathbf{J}^T\mathbf{C}_D^{-1}\mathbf{J} + \alpha\mathbf{D}^T\mathbf{D}\right]^{-1}\mathbf{J}^T\mathbf{C}_D^{-1}\mathbf{J}. \quad (5)$$

Therefore,

$$\hat{\mathbf{m}} = \mathbf{R}\,\mathbf{m}_{true} + \left(\mathbf{I} - \mathbf{R}\right)\mathbf{m}_{prior} \quad (6a)$$

where $\mathbf{I}$ is the identity matrix. Commonly, the prior model is spatially uniform. Under these conditions, equation 6a becomes

$$\hat{\mathbf{m}} = \mathbf{R}\,\mathbf{m}_{true}. \quad (6b)$$

For linear problems, where the elements of $\mathbf{J}$ are independent of the values of $\mathbf{m}_{true}$, $\mathbf{R}$ can be calculated prior to data collection. For non-linear problems, $\mathbf{R}$ can be calculated using the $\mathbf{J}$ and α from the last iteration of the inversion, and equation (6b) becomes approximate [e.g., *Alumbaugh and Newman*, 2000]. Since the model resolution matrix describes the loss of resolution incurred during a geophysical survey, it is a quantitative representation of the geophysical filter. According to equation (6), tomographic estimates can be interpreted as weighted averages of the true values of the imaged property, where the weights are described by the rows of R:

$$\hat{m}_i = \sum_{j=1}^{n} R_{ij} m_j^{true}. \quad (7)$$

In general, tomograms exhibit smaller variance and greater correlation lengths than the underlying property, and this distortion tends to be anisotropic and non-stationary (Plate 1). Because the correlation between point-scale measurements of hydrologic and geophysical properties is degraded by the inversion process (which may be quantifiable through $\mathbf{R}$ in certain circumstances), the use of standard petrophysical relations with field-scale tomograms may not be appropriate. *Cassiani et al.* [1998] noted correlation loss between tomographic estimates of seismic velocity and hydraulic conductivity in poorly resolved regions of tomograms. In an ERT study to monitor a fluid tracer in the unsaturated zone, *Binley et al.* [2002] applied locally derived petrophysical relations to convert resistivity tomograms to changes in moisture content; their analysis revealed a 50% mass balance error that was attributed to the poor sensitivity in the center of the image volume where the tracer was applied. In an effort to monitor tracer experiments with ERT, *Singha and Gorelick* [2005] noted the impact of regularization and inversion artifacts on the estimated tracer mass and spatial variance, and demonstrated that Archie's law failed to accurately reproduce solute concentrations without consideration of resolution.

2.3. New Approaches to Field-Scale Petrophysics

Because of issues associated with poor geophysical resolution and limited collocated data, numerous scientists have attempted to develop a correction that could be applied to their geophysical data. *McKenna and Poeter* [1995] noted weak correlation between tomographic estimates of seismic velocity and collocated measurements of hydraulic conductivity compared to the correlation seen for higher resolution sonic logs; they derived a correction based on regression

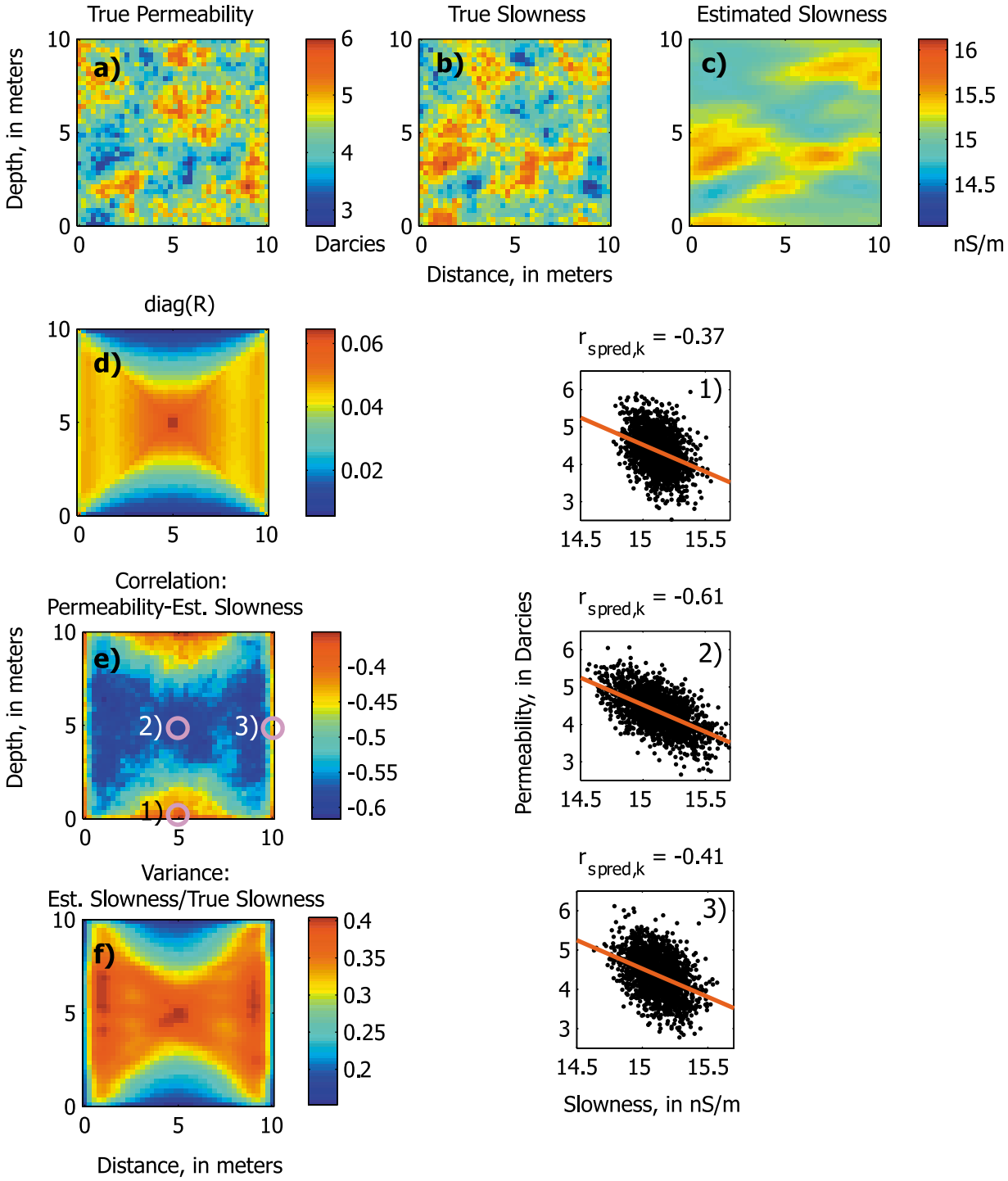

Plate 1. Radar travel time tomography for a field where a linear correlation with permeability is assumed. Cross sections of (a) true permeability; (b) true slowness; (c) inverted tomogram of slowness; (d) diagonal of the model resolution matrix; (e) the predicted correlation coefficient between true and estimated slowness; and (f) the predicted variance of the inverted tomogram normalized by the variance of the true slowness. Three pixels in the correlation coefficient matrix are highlighted [(1), (2), and (3)], showing that the estimated relation between permeability and slowness is spatially dependent.

and applied the correction uniformly over the tomogram to correct for the correlation loss between velocity and hydraulic conductivity. *Hyndman et al.* [2000] used an approach that combined geostatistical simulation, flow and transport simulation, and regression methods to calibrate a linear, field-scale relation between estimated seismic slowness and the logarithm of hydraulic conductivity. *Mukerji et al.* [2001] provided a framework for "statistical" petrophysics to account for conditions not explicitly represented in a data set with limited collocated measurements. In their approach, fluid saturations that were not directly observed at a well location but were likely to occur in the subsurface were included in the calibration data set. They did this by using Gassmann's relation [1951] to predict the change in seismic velocity for a given change in saturation. An assumption in these approaches is that the resulting petrophysical relations are not dependent on spatial location within the subsurface; recent theoretical work by *Day-Lewis and Lane* [2004], however, indicates that this assumption is often not appropriate.

2.3.1 Random field averaging approach. Day-Lewis and Lane [2004] developed an analytical method to determine the correlation loss between hydrological and geophysical measurements as a function of measurement physics, survey geometry, measurement error, spatial correlation structure of the subsurface, and regularization. This was accomplished by combining random field averaging (RFA) [*VanMarcke*, 1983], which allows calculation of the statistical properties of weighted averages of random functions, and the definition of the model resolution matrix (equation 6b).

As shown previously, tomographic estimates can be interpreted as weighted averages of point-scale properties. Estimating pixel values as a weighted average using equation (7), applying the random field average of *VanMarcke* [1983], making a Markov-type approximation [*Journel*, 1999], and calculating the cross-covariance between the geophysical parameter, m, and the hydrologic parameter of interest, p, we find:

$$\hat{\sigma}^2_{\hat{m}_i} = \sum_{j=1}^{N}\sum_{k=1}^{N} R_{ij}R_{ik}\sigma_{m_j,m_k}, \tag{8}$$

$$\hat{\sigma}_{\hat{m}_i,\hat{m}_k} = \sum_{j=1}^{N}\sum_{l=1}^{N} R_{ij}R_{kl}\sigma_{m_j,m_l}, \tag{9}$$

$$\hat{r}_{\hat{m}_i,p_i} = \frac{\sigma_{\hat{m}_i,p_i}}{\sqrt{\sigma^2_{\hat{m}_i}\sigma^2_{p_i}}} \approx r_{m,p}\hat{r}_{m_i,\hat{m}_i} = r_{m,p}\sum_{j=1}^{N} R_{ij}\sigma_{m_i,m_j} \Big/ \sqrt{\sigma^2_m\hat{\sigma}^2_{\hat{m}_i}}. \tag{10}$$

where $\sigma_{x,y}$ is the covariance between variables x and y where x or y may be m and $\hat{m}$ or p;

σ^2_x is the variance of variable x; and

$r_{x,y}$ is the correlation coefficient between collocated values of x and y at the point scale.

These equations allow us to predict the variance reduction of the pixel-scale tomographic estimate ($\hat{m}_i$) compared to the point-scale property (m_i) (equation 8), the spatial covariance of the tomogram (equation 9), and the correlation loss between the tomographic estimate ($\hat{m}_i$) and collocated hydrologic property p_i (equation 10). Figure 1 shows a flowchart of this approach, which involves seven steps:

1. *Construction of "small-scale" hydrogeologic property realizations:* A realization of the geophysical parameter is generated, assuming a known covariance structure and second-order stationarity.
2. *Application of petrophysical relation:* Site-specific laboratory measurements and/or petrophysical theories are used to generate a field of the hydrologic property of interest, from the realization of the geophysical parameter.
3. *Geophysical forward modeling:* Synthetic geophysical data are calculated using an analytical or numerical model for the measurement physics and survey geometry. Given a model of expected measurement errors, random errors may be added to the data.
4. *Geophysical inverse modeling:* The synthetic measurements obtained via forward modeling in step 3 are inverted.
5. *Random Field Averaging (RFA)*: The RFA equations (Equations 8–10) are applied to predict the parameters describing the pixel-specific statistical distributions of the estimated geophysical parameter.
6. *Construct Bivariate Probability Distribution Functions (PDFs) between True and Estimated Geophysical Parameters:* Assuming Gaussian distributions, we construct bivariate probability distribution functions between the true and estimated geophysical parameters.
7. *Application of petrophysical relation:* Using the petrophysical relation from step 2, we convert the PDF from step 6 to a bivariate PDF between the estimated geophysical parameter and true hydrologic parameter.

For the simplified case of linear, straight-ray radar tomography and linear correlation between radar slowness (1/velocity) and the natural logarithm of permeability, *Day-Lewis and Lane* [2004] derived formulas to predict 1) how the inversion process degrades the correlation between imaged slowness and permeability, compared to point measurements; 2) how the variance of the estimated slowness compares to the variance of the true slowness; and 3) how the inversion alters the spatial covariance of the estimated slowness. This work was expanded in *Day-Lewis et al.* [2005] to consider non-linear tomographic inversion and non-linear petrophysi-

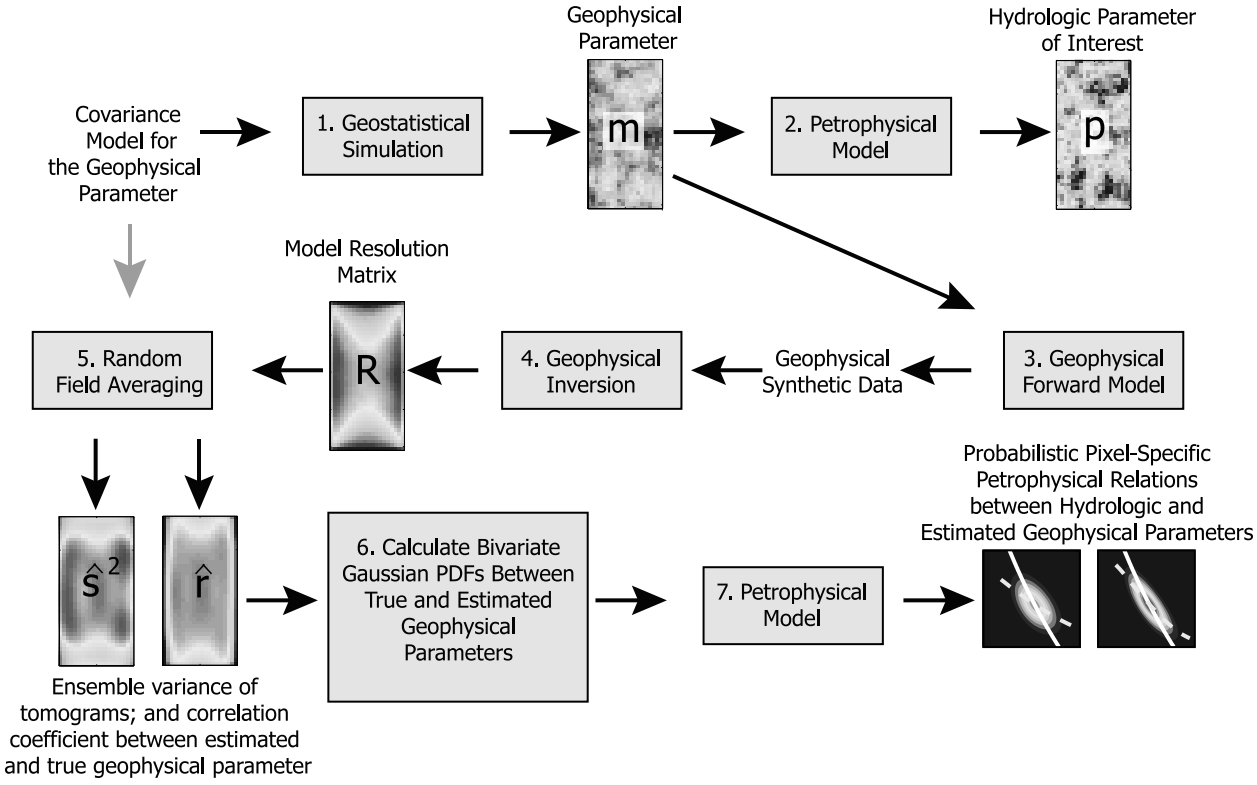

Figure 1. Flowchart for Random Field Averaging Analysis. Starting from an assumed covariance describing the spatial structure of the geophysical parameter, a realization is generated and converted using the petrophysical model to the hydrologic property of interest. Synthetic geophysical data are calculated in the next step. Then the data are inverted and the model resolution matrix calculated. Random field averaging is used to upscale the spatial covariance based on the model resolution matrix and to calculate (1) the ensemble variance of the estimated geophysical parameter and (2) the correlation coefficient between the estimated and true geophysical parameters. Based on these results, bivariate probability distribution functions between the true and estimated geophysical parameter are calculated. In the final step, the bivariate distributions are transformed using the petrophysical model to yield pixel-specific petrophysical relations. Adapted from Day-Lewis et al. [2005].

cal relations. In this later work, patterns of correlation loss and variance reduction for both ERT and fresnel-volume, or "fat ray", radar-traveltime tomography were investigated. In this case, because the petrophysical relations are non-linear, a more flexible approach was used, which considers the relation between the true and estimated geophysical parameter; the petrophysics was applied afterward to estimate hydrologic properties. The authors found that while ERT generally performs better near boreholes, where the electrodes were located, and radar-traveltime tomography performs better in the interwell region, the degradation in the relation between the geophysical and hydrologic property is a function of multiple factors: subsurface heterogeneity, the regularization used in the inverse problem, and the number and geometry of data collected. Consequently, imaging targets in the field is dependent on the distance of the targets from the electrodes, the number of data and the geometry with which they are collected, and the type of smoothing used to obtain convergence in the geophysical inverse problem.

The principal benefits of the RFA approach are that 1) it is semi-analytical and therefore provides clear insights into how choices of survey geometry, inversion parameters, or regularization criteria impact the use of tomograms for hydrologic estimation; and 2) it is no more CPU-intensive than the resolution modeling performed as part of a rigorous analysis of tomographic data.

Several key issues limit the applicability of the RFA approach. Whereas the RFA equations provide a semi-analytical way to estimate the degradation in the relation between hydrologic and geophysical parameters, the approach is based on a number of assumptions that may limit its utility to field applications, including: 1) the geophysical parameter is normally distributed, 2) both the geophysical and hydrologic properties share the same covariance struc-

ture, and 3) both properties are second-order stationary, i.e., the mean and variance are spatially uniform and the covariance between two points depends only on the separation between them.

2.3.2 Full inverse statistical calibration. An alternative approach to accounting for geophysical resolution in petrophysical relations is to generate a large number of subsurface property realizations, forward model and invert the tomographic experiment for each realization, and finally compare the resulting tomograms with the original realizations to assess the impact of the geophysical filter. *Moysey et al.* [2005] and *Singha and Moysey* [2006] give examples where this type of a numerical simulation approach is used to capture the spatial variability in resolution of geophysical surveys. The method is referred to as Full Inverse Statistical (FISt) calibration because a full forward and inverse simulation must be performed for each realization used in the calibration (or statistical inference) of the field-scale petrophysical relation. The approach used by these authors follows a six-step process, and is outlined schematically in a flowchart in Figure 2:

1. *Construction of "small-scale" hydrogeologic property realizations:* A set of realizations of the hydrogeologic property of interest is created using a technique that honors both the available data and conceptual model for the field site, e.g., geostatistical simulation or flow and transport modeling. These realizations should be simulated at an appropriate scale such that small-scale heterogeneities, should they be known, can be captured by effective parameters, but larger-scale heterogeneities affecting hydrologic (or geophysical) behavior are explicitly represented.
2. *Application of a traditional petrophysical relation:* Site-specific laboratory measurements and/or petrophysical theories are used to determine relations between the hydrogeologic and geophysical properties under investigation. Geophysical property realizations can then be obtained from the hydrogeologic property realizations generated in step 1 using this relation.
3. *Geophysical forward modeling:* A numerical analog to the experiment executed in the field is performed on each geophysical property realization from step 2. The numerical experiment should parallel as closely as possible the real field experiment in both experimental design (e.g., survey geometry, data acquisition parameters) and representation of the relevant physical processes.
4. *Geophysical inverse modeling:* The synthetic measurements obtained via forward modeling in step 3 are then inverted for each realization. The forward and inverse geophysical model need not use the same grid; in fact, doing so assumes that there are no subgrid-scale heterogeneities impacting the data. The inversion of the measurements into tomograms mimics the inversion of the field data, including the parameterization (i.e., model grid) and selection of regularization criteria. The goal is to reproduce the processing and inversion steps that have been applied to the field measurements.
5. *Generation of field-scale hydrogeologic property realizations*: Each hydrogeologic property realization is upscaled to the model grid selected in step 4 using an appropriate spatial weighting function. For example, if hydrogeologic properties of interest are volumetric properties, e.g., water content, this step can be carried out using volumetric averaging.
6. *Development of "apparent" or field-scale petrophysical relations:* The sets of field-scale hydrogeologic analogs from step 5 and geophysical analogs from step 4 are used to calculate the apparent petrophysical relation at every location in space (as defined by a pixel or voxel). The petrophysical relations should also be updated for each observation time during a monitoring experiment. The resulting relations can then be used to post-process the real-world geophysical properties to obtain an estimate of the hydrogeologic properties for the actual field site.

One final practical consideration in implementing FISt calibration is the decision of how to find the best-fit line between the geophysical and hydrologic property for each pixel. There are many different means of obtaining a best-fit line. The most obvious choice, least-squares regression, produces a result that depends on which variable is considered independent—the best-fit linear relation of permeability versus velocity may be quite different from that of velocity vs. permeability. Ideally with FISt, we want to find the relation that allows the estimated and "true" property, permeability in this case, to fall on a 1:1 line. One way to do this is to regress both the x and y axes and minimize the sum of squares of the perpendicular distances from the line, i.e., major-axis regression. Another possibility is to consider a distribution transformation:

$$Y = \sigma_Y \left(\frac{X - \mu_X}{\sigma_X} \right) + \mu_Y \tag{11}$$

In theory, the field-scale petrophysical relation determined at each spatial location could be a non-parametric estimate of the joint probability density function (PDF) between the geophysical and hydrologic parameters of interest. In practice, such inference would require a large number of simulations to be performed. When the full joint PDF is not needed, e.g., if a multi-modal PDF is not of concern, it is more practical to fit a simple model (e.g., linear relation) at each spatial location using a limited number of realizations.

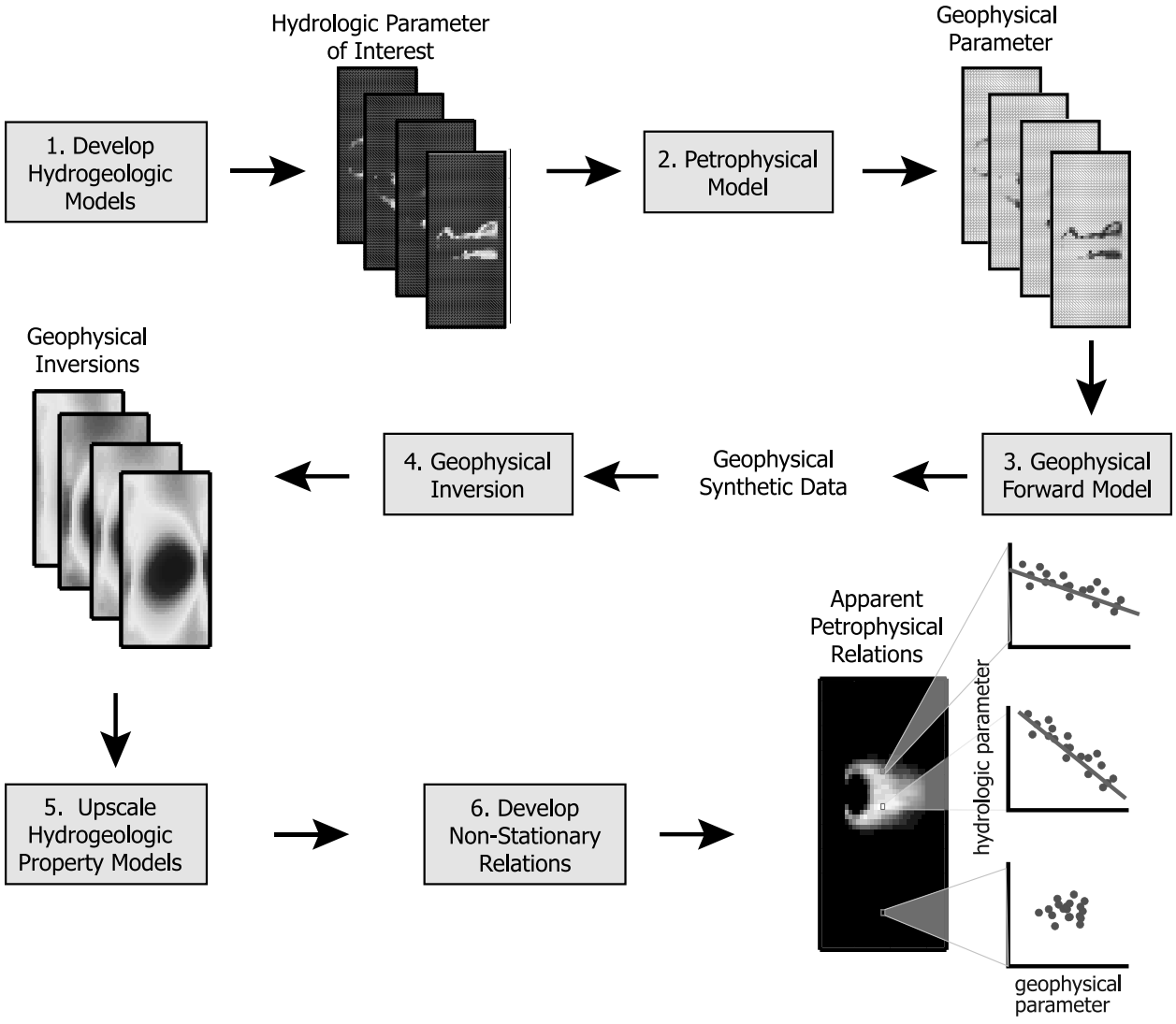

Figure 2. Flowchart for FISt calibration. Realizations of hydrologic properties can be generated by geostatistical calibration, flow and transport models, or from conceptual understanding of field sites. These realizations are converted to geophysical properties through a petrophysical relation. Following this step, forward and inverse geophysical simulations are conducted. By considering multiple realizations, relations are then built between the inverted geophysical parameter and the hydrologic parameter at every pixel to account for spatially variable resolution. These relations are applied to an inversion of field geophysical data for a better estimation of hydrologic properties than otherwise attainable. Adapted from Moysey et al. [2005] and Singha and Gorelick [2006].

In 2D synthetic examples, *Moysey et al.* [2005] and *Singha and Moysey* [2006] used FISt calibration to improve estimates of water content and solute concentration for radar traveltime and ERT experiments, respectively. Extending this work to a 3D transient system in the field, *Singha and Gorelick* [2006] applied a similar approach to ERT monitoring of a tracer test performed at the Massachusetts Military Reservation, Cape Cod, Massachusetts. The tracer concentrations and total solute mass estimated from the ERT survey were in better agreement with multi-level sampler results when the authors used field-scale petrophysical relations rather than Archie's law to convert resistivity to concentration. *Singha and Gorelick* [2006] also demonstrated that rather than develop "apparent" petrophysical relations between a hydrologic and geophysical property, FISt can also be used to "correct" tomograms by building relations between the true and estimated geophysical property. The benefit of comparing the true and estimated geophysical

parameter, rather than converting to a hydrologic parameter, is that the relation between them is likely to be well-described by a bivariate normal distribution that can be captured in a linear relation.

One benefit of FISt calibration is that it is conceptually straightforward to implement. Another strength of this method is that it is easy to account for different kinds of uncertainty within the Monte Carlo-type framework of the method. For example, if the hydrologic conceptual model at a site is considered uncertain, it is straightforward to implement FISt calibration using realizations based on different conceptual models or generated using different simulation techniques. This degree of flexibility makes the method potentially quite powerful. A third advantage of the FISt approach is the capability to condition to secondary information, e.g., direct point measurements of the geophysical or hydrologic properties under investigation.

There are at least three key issues that should be considered when using FISt calibration: 1) a meaningful relation between the geophysical and hydrologic parameters, 2) the appropriateness of the realizations used in the simulations with respect to the field-site hydrogeology, and 3) the ability of the numerical models used in the forward simulations to adequately capture 'real-world' processes. The lack of geophysical data sensitivity to the hydrologic properties of interest, i.e., non-informative data, is a general problem that will defeat any approach to data integration. The second and third issues, however, are important considerations that can potentially lead to biased estimates of the resulting field-scale petrophysical relation, and therefore, inaccurate estimates of hydrologic properties. An additional consideration in using FISt calibration is that it is computationally expensive, especially for 3D transient problems.

Both FISt calibration and the RFA-based approach are similar to traditional petrophysics in that they use a mathematical (or numerical) model to describe how geophysical measurements sample the subsurface. In contrast to traditional approaches, however, these methods also account for the impacts of inversion on geophysical resolution rather than focusing on how a single measurement averages the subsurface. Both the RFA method and FISt calibration can determine the petrophysical relation between a geophysical and hydrologic variable as a statistical association, captured by a PDF that is explicitly dependent on spatial location, therefore inherently accounting for the spatially varying resolution of geophysical surveys. The overall conceptual similarity between the two approaches is made apparent by comparing the flowcharts in Figures 2 and 3. The main difference between the two approaches is that RFA is a semi-analytical approach that relies on an assumption of second-order stationary distributions, whereas FISt calibration is a non-parametric, numerical approach that allows for any model of spatial variability. In summary, the RFA method will typically be more computationally efficient, but the flexibility of FISt calibration makes it more generally applicable.

3. EXAMPLE

We demonstrate the utility of FISt and RFA for a synthetic example where radar slowness is considered to be linearly related to permeability. Although FISt has been used in the past to convert tomograms to hydrologic estimates, RFA has not; RFA has been used only to predict the loss of information arising from limited survey geometry, regularization criteria, measurement errors, and other factors that affect tomographic resolution. Here, we demonstrate how the field-scale petrophysical relations generated with RFA can be used to produce more reliable hydrologic estimates from tomograms.

Our example assumes a linear relation with a correlation coefficient of -0.9 between radar slowness and permeability. There have been examples where similar relations were assumed to be valid [e.g., *Hubbard et al.*, 1997; *Linde et al.*, 2006]; we note, however, that such a linear model may only be hypothetical, with limited realism in many or most field scenarios, and should be applied in the field only with great care. Correlated permeability and slowness fields (Figure 3a, b, respectively) are generated using sequential Gaussian simulation with an exponential covariance model, assuming an isotropic correlation length of 2.5 m, mean ln$k$ [darcies] of 4.35, variance of ln$k$ of 0.25, mean radar slowness of 15.12 ns/m, and variance of radar slowness of 0.0973 ns^2/m^2. Radar traveltimes are calculated assuming straight raypaths, for 1600 measurements with antenna spacings of 0.25 m along each 10-m deep borehole. The grids for forward simulation and tomographic inversion are identical, with a discretization of 0.25-m square pixels. For simplicity, we assume straight rays for forward modeling traveltimes. More sophisticated eikonal-solver forward models have been considered in other applications [*Day-Lewis et al.*, 2005; *Moysey et al.*, 2005]; however, for our present purpose of comparing FISt and RFA for linear problems, straight rays are appropriate and sufficient. The measurement errors are assumed to be normally distributed with zero mean and standard deviation of 2.0 ns (1.5%); this standard error is large relative to common sampling periods, but is intended to represent the combined effects of errors in traveltime picking, inaccurate borehole deviation and antenna positions, and modeling errors arising from the straight-ray approximation. It should be noted that errors are considered independent in this synthetic example, but are likely correlated in real field data. The inverse model

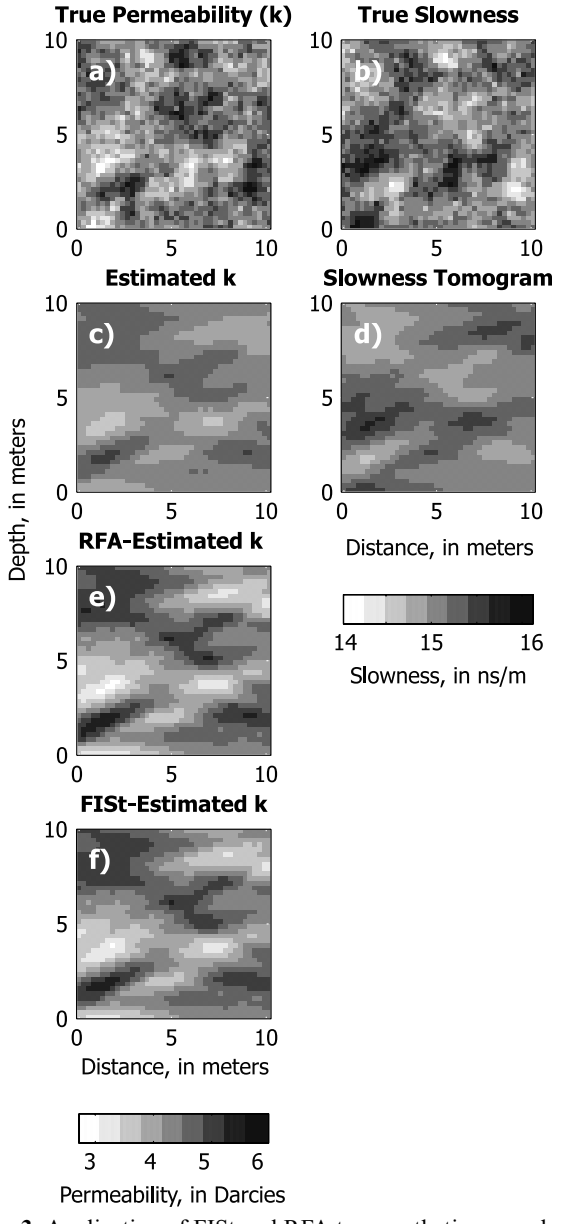

Figure 3. Application of FISt and RFA to a synthetic example of estimating permeability from crosswell radar data, where (a) is the true permeability and (b) is the true slowness. Shown are the (c) estimated permeability and (d) slowness distributions obtained using inversion and the application of our assumed relation; (e) the estimation of permeability using RFA; and (f) the estimation of permeability using FISt.

is linear and amounts to a single iteration of equations (2–3), with $\mathbf{J}_{ij}$ equal to the length of raypath i in pixel j.

Compared to the true slowness field (Figure 3b), the tomogram (Figure 3d) is smoother and shows less variation in slowness. The tomography resolves only large-scale structures and even these are smeared or blunted. The differences between true and estimated slowness arise because of measurement errors, the limited data collection geometry, and regularization; therefore, after tomographic reconstruction, the relation between true permeability and estimated slowness varies within the tomogram as a function of the spatial variability in resolution. Consequently, any estimation of permeability from radar data is biased, even in this simple synthetic example where a strong correlation between permeability and slowness exists. To demonstrate the degree of bias, we use the linear relation between true slowness and permeability to convert the tomogram to a cross-section of permeability estimates (Figure 3c), and plot the permeability estimates against true, synthetic permeability (Figure 4a). High values of permeability are underestimated and low values are overestimated; the loss of extreme values is clearly evident in quantile-quantile comparison between estimated and true permeability (Figure 4d).

Correction of the tomogram with FISt and RFA shows that accounting for spatial variability can improve the estimation of permeability values without greatly impacting the fit to the data (Figure 3e, f; Table 1). To create the slope and

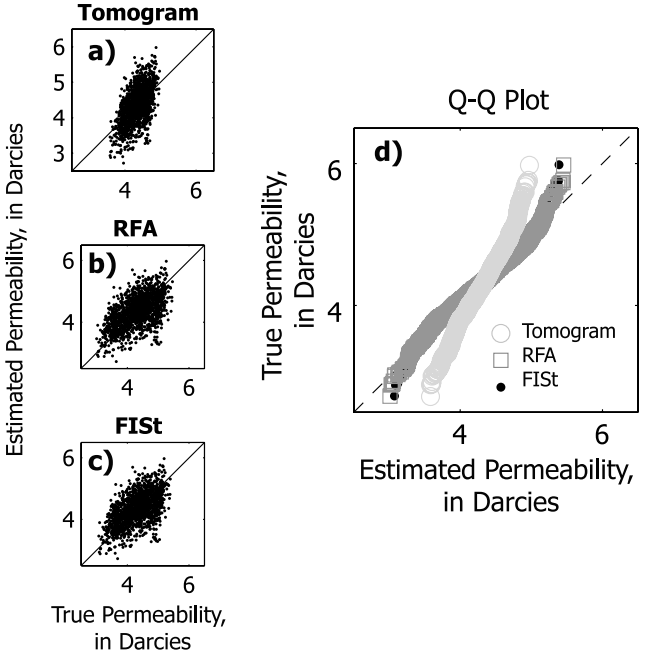

Figure 4. Plots of true versus estimated permeability illustrate the accuracy of the estimates obtained using: (a) tomographic inversion and application of "true" relation, (b) RFA, and (c) FISt; accurate estimates fall along the 1:1 line. The (d) Q-Q plot, which compares the quantiles of the distributions of the true versus estimated permeabilities, shows that the estimate from tomographic inversion significantly underestimates the true permeability. Both RFA and FISt match the permeabilities in the central quartiles, but still underestimate the extremes.

Table 1. Estimates of correlation between true and estimated permeability over the entire tomogram, the RMS error associated with the slowness tomograms versus the original field, the forward-modeled data misfit associated with the slowness tomogram, and the fraction of the variance in the slowness tomogram compared to the original slowness field.

	k-k Correlation	RMS Error	Data Misfit	Fraction of True Variance
Original Tomogram	0.577	0.408	0.996	0.299
FISt-corrected	0.562	0.460	1.03	0.94
RFA-corrected	0.560	0.476	1.05	1.07

intercept maps for both FISt and RFA, we transformed the distribution of slowness to the natural logarithm of permeability assuming both to be normal—while this assumption may not always be appropriate in the field, it is applicable for this example. The updated cross sections of permeability show increased variance; areas of high and low slowness (and permeability) are better captured in the RFA and FISt estimates (Figure 3e, f) than in the original tomogram. The RMS error and overall correlation between true and estimated slowness are slightly poorer than in the original tomogram; however, these metrics may be less important to a hydrogeologist than capturing the tails of the permeability distribution. While the correlation between the true and estimated permeability does not markedly increase (Figure 4b, c), the scatter better fits the 1:1 line than the original tomogram, and the variance in the permeability is greatly improved, as illustrated in quantile-quantile plots (Figure 4d). Improved mapping of the high and low permeabilities in the field, should a relation between permeability and slowness exist, would be critical to understanding flow and transport processes in a given setting.

4. DISCUSSION

FISt calibration and RFA provide improved methods for estimating hydrologic properties (in this case, permeability) from geophysical data, should the relation between the geophysics and hydrogeology exist. Both perform equally well for the example presented; however, both have important limitations when being applied to field data. First and foremost, both require that a relation between the geophysical and hydrologic property exists. While this relation is relatively clear in some circumstances (changes in water content or total dissolved solids and electrical resistivity, for instance), estimation of static properties such as permeability or the concentration of a dissolved non-aqueous phase liquid at some time may be impossible for geophysical methods to image directly. An assumption of correlation between hydrologic and geophysical parameters that does not exist may lead one to believe that geophysical methods can be used to estimate hydrologic processes when the geophysical data are actually uninformative. Another major issue is the sensitivity of the tomogram appearance to the final RMS error. Both methods may overpredict the hydrologic property if the data are overfitted, which could happen with the translation of geophysical tomograms to hydrologic data given standard petrophysical relations. It is similarly important that all the inversions for the numerical analogs used in FISt and the field data converge to similar error levels. If the data are over- or underfitted, the final tomograms exhibit different degrees of spatial variation; consequently the apparent petrophysical relations may not be meaningful.

The RFA approach depends only on the resolution matrix and covariance models to estimate correlation loss. Numerous studies, however, have indicated that two-point statistics, or covariance models, are inappropriate for generating realistic connectivity in highly heterogeneous media [e.g., *Western et al.*, 1998; *Caers et al.*, 2003; *Zinn and Harvey*, 2003; *Knudby and Carrera*, 2005]. While RFA is more mathematically rigorous than FISt, it is unlikely to be used to correct tomograms in the field, as the assumption of second-order stationarity is unlikely to be valid. FISt therefore has a wider applicability in real-world scenarios, where objects such as plumes, which are not easily described by two-point statistics, may be the target of interest. Additionally, RFA may prove to be limited in cases of highly nonlinear physics. The calculation of **R** in nonlinear methods is local to the final solution; for mild non-linearity, the resolution will be relatively stable, but this may not be the case in the presence of high velocity contrasts. This limitation has the potential to impact the applicability of RFA to some scenarios.

While FISt has the advantage of not being limited by a covariance model, the method is computationally expensive, and like other Monte Carlo methods may require many hundreds or thousands of inversions to obtain good results [*Peck et al.*, 1988]. FISt is also model-dependent, and requires an estimate of the subsurface properties to build the calibration relations. While we often have more data about our field sites than are used in inversion (a geologist's rendition of the field area, for instance), we must attempt to minimize the introduction of features that are unlikely to exist—a poor choice for the underlying hydrogeology in construction of the realizations can cause spurious results [*Singha and Gorelick*, 2006]. Another issue with FISt is that the pixels or voxels

are also assumed to be independent, which is not true; they are dependent upon the resolution of the inverse procedure. Each estimated parameter is dependent upon the surrounding model space as dictated by the Backus and Gilbert averaging kernel [*Backus and Gilbert*, 1968]. This is not a concern for RFA, which uses the entire resolution matrix when calculating relations. A strength of FISt, however, is that it remains applicable with nonlinear inversion [e.g., *Singha and Gorelick*, 2006; *Singha and Moysey*, 2006].

While these methods can be used in the "design" phase of a survey to assess a priori the nature of the resulting, space-dependent, constitutive models, they can also be used to estimate hydrologic properties a posteriori from field data by developing petrophysical models specific to given acquisition geometries and local geology. Despite the complications above, both of these methods provide improved estimates of hydrologic properties and processes when applied with care, and also allow for quantification of the correlation loss between geophysical properties measured in the field, and hydrologic properties of interest, either before entering the field, or once data have been collected.

5. CONCLUSIONS

Geophysical tomograms are plagued by spatially variable resolution, making the estimation of hydrologic properties from them a difficult task. We have presented two methods currently available for mitigating these problems: FISt and RFA. Both have distinct advantages and disadvantages. While RFA provides a semi-analytical way to quantify spatially variable correlation loss, it is limited by the requirement of a known covariance model. FISt, on the other hand, is applicable in situations where two-point statistics may not be valid (the movement of contaminant plumes or infiltration), but is computationally expensive because of the number of realizations that must be considered; FISt (as described here) assumes a linear model between parameters and pixel independence. Nevertheless, both of these methods provide a manner for estimating spatially variable petrophysical relations applicable in field settings, to improve quantification of hydrologic properties and processes from geophysical data.

Acknowledgments. Aspects of this work were funded by the National Science Foundation (awards EAR-0229896 and EAR-012462) and the U.S. Geological Survey Toxics Substances Hydrology Program. The authors are grateful for useful comments from John W. Lane, Jr., James Irving, and Adam Pidlisecky. Any opinions, findings, and conclusions or recommendations expressed in this material are those of the authors and do not necessarily reflect the views of the National Science Foundation.

REFERENCES

Alumbaugh, D. L., P. Y. Chang, L. Paprocki, J. R. Brainard, R. J. Glass and C. A. Rautman, Estimating moisture contents in the vadose zone using cross-borehole ground penetrating radar: a study of accuracy and repeatability, *Water Resources Research,* 38(12): 1309, doi: 10.1029/2001/WR000754, 2002.

Alumbaugh, D. L. and G. A. Newman, Image appraisal for 2-D and 3-D electromagnetic inversion, *Geophysics,* 65(5): 1455–1467, 2000.

Archie, G. E., The electrical resistivity log as an aid in determining some reservoir characteristics, *Transactions of the American Institute of Mining, Metallurgical and Petroleum Engineers,* 146: 54–62, 1942.

Backus, G. E. and J. F. Gilbert, The resolving power of gross earth data, *Geophysical Journal of the Royal Astronomical Society,* 16: 169–205, 1968.

Berge, P. A., J. G. Berryman and B. P. Bonner, Influence of microstructure on rock elastic properties, *Geophysical Research Letters,* 20: 2619–2622, 1993.

Berthold, S. and L. R. H. Masaki, Integrated hydrogeological and geophysical study of depression-focused groundwater recharge in the Canadian prairies, *Water Resources Research,* 40(6): doi:10.1029/2003WR002982, 14p., 2004.

Binley, A., G. Cassiani, R. Middleton and P. Winship, Vadose zone flow model parameterisation using cross-borehole radar and resistivity imaging, *Journal of Hydrology,* 267: 147–159, 2002.

Blair, S. C. and J. G. Berryman, Permeability and relative permeability in rocks, *Fault Mechanics and Transport Properties of Rocks*, Academic Press Ltd.: . 169–186, 1992.

Caers, J., S. Strebelle and K. Payrazyan, Stochastic integration of seismic data and geologic scenarios, *The Leading Edge,* 22(3): 192–196, 2003.

Carle, S. and A. Ramirez, *Integrated Subsurface Characterization Using Facies Models, Geostatistics, and Electrical Resistance Tomography* Lawrence Livermore National Laboratory, UCRL-JC-136739, Livermore CA, 1999.

Cassiani, G., G. Böhm, A. Vesnaver and R. Nicolich, A Geostatistical Framework for Incorporating Seismic Tomography Auxiliary Data into Hydraulic Conductivity Estimation, *Journal of Hydrology,* 206(1-2): 58–74, 1998.

Chan, C. Y. and R. J. Knight, Determining water content and saturation from dielectric measurements in layered materials, *Water Resources Research,* 35(1): 85–93, 1999.

Dahlen, F. A., Resolution limit of traveltime tomography, *Geophysical Journal International,* 157: 315–331, doi:10.1111/j.1365-246X.2004.02214.x, 2004.

Day-Lewis, F. D. and J. W. Lane, Jr., Assessing the resolution-dependent utility of tomograms for geostatistics, *Geophysical Research Letters,* 31: L07503, doi:10.1029/2004GL019617, 2004.

Day-Lewis, F. D., K. Singha and A. M. Binley, Applying petrophysical models to radar traveltime and electrical-resistivity tomograms: resolution-dependent limitations, *Journal of Geophysical Research,* 110: B08206, doi:10.1029/2004JB003569, 2005.

Dietrich, P., T. Fechner, J. Whittaker and G. Teutsch, *An integrated hydrogeophysical approach to subsurface characterization*, GQ 98 conference, Tubingen, Federal Republic of Germany, [Louvain] : International Association of Hydrological Sciences, 513–519, 1998.

Doyen, P. M., Porosity from seismic data; a geostatistical approach, *Geophysics,* 53(10): 1263–1276, 1988.

Dunn, K.-J., G. A. LaTorraca and D. J. Bergman, Permeability relation with other petrophysical parameters for periodic porous media, *Geophysics,* 64(2): 470–478, 1999.

Friedel, S., Resolution, stability, and efficiency of resistivity tomography estimated from a generalized inverse approach, *Geophysical Journal International,* 153: 305–316, 2003.

Gal, D., J. Dvorkin and A. Nur, A physical model for porosity reduction in sandstones, *Geophysics,* 63(2): 454–459, 1998.

Gassmann, F., Elastic waves through a packing of spheres, *Geophysics,* 16(673–685), 1951.

Hashin, Z. and S. Shtrikman, A variational approach to the theory of effective magnetic permeability of multiphase materials, *Journal of Applied Physics,* 33: 3125–3131, 1962.

Hashin, Z. and S. Shtrikman, A variational approach to the elastic behavior of multiphase materials, *J. Mech. Phys. Solids,* 11: 127–140, 1963.

Hubbard, S. S., J. Chen, J. Peterson, E. L. Majer, K. H. Williams, D. J. Swift, B. Mailloux and Y. Rubin, Hydrogeological characterization of the South Oyster Bacterial Transport Site using geophysical data, *Water Resources Research,* 37(10): 2431–2456, 2001.

Hubbard, S. S., J. E. Peterson, Jr., E. L. Majer, P. T. Zawislanski, K. H. Williams, J. Roberts and F. Wobber, Estimation of permeable pathways and water content using tomographic radar data, *The Leading Edge,* 16(11): 1623–1628, 1997.

Hunt, A. G., Continuum percolation theory and Archie's Law, *Geophysical Research Letters,* 31(19): L19503, 10.1029/2004GL020817, 2004.

Hyndman, D. W. and S. M. Gorelick, Estimating lithologic and transport properties in three dimensions using seismic and tracer data; the Kesterson Aquifer, *Water Resources Research,* 32(9): 2659–2670, 1996.

Hyndman, D. W., J. M. Harris and S. M. Gorelick, Coupled seismic and tracer test inversion for aquifer property characterization, *Water Resources Research,* 30(7): 1965–1977, 1994.

Hyndman, D. W., J. M. Harris and S. M. Gorelick, Inferring the relation between seismic slowness and hydraulic conductivity in heterogeneous aquifers, *Water Resources Research,* 36(8): 2121–2132, 2000.

Jorgensen, D. G., Estimating permeability in water-saturated formations, *Log Analyst,* 29(6): 401–409, 1988.

Journel, A. G., Markov models for cross-covariances, *Mathematical Geology,* 31: 955–964, 1999.

Kelly, W. E., Geoelectric sounding for estimating aquifer hydraulic conductivity, *Ground Water,* 15(6): 420–425, 1977.

Klimentos, T. and C. McCann, Relationships among compressional wave attenuation, porosity, clay content, and permeability in sandstones, *Geophysics,* 55(8): 998–1014, 1990.

Knight, R. J. and A. L. Endres, Physical properties of near-surface materials and approaches to geophysical determination of properties, *Near-Surface Geophysics, Volume 1*, editors. Tulsa, OK, Society of Exploration Geophysicists: 723 pp., 2005.

Knudby, C. and J. Carrera, On the relationship between indicators of geostatistical, flow, and transport connectivity, *Advances in Water Resources,* 28: 405–421, 2005.

Kowalsky, M. B., S. Finsterle, J. Peterson, S. Hubbard, Y. Rubin, E. Majer, A. Ward and G. Gee, Estimation of field-scale soil hydraulic and dielectric parameters through joint inversion of GPR and hydrological data, *Water Resources Research,* 41(W11425, doi:10.1029/2005WR004237), 2005.

Linde, N., S. Finsterle and S. Hubbard, Inversion of tracer test data using tomographic constraints, *Water Resources Research,* 42(4): W04410, 10.1029/2004WR003806, 2006.

McKenna, S. A. and E. P. Poeter, Field example of data fusion in site characterization, *Water Resources Research,* 31(12): 3229–3240, 1995.

Menke, W., *Geophysical data analysis; discrete inverse theory*, New York-London-Toronto, Academic Press, 289, 1984.

Moysey, S. and R. J. Knight, Modeling the field-scale relationship between dielectric constant and water content in heterogeneous systems, *Water Resources Research,* 40: W03510, doi:10.1029/2003WR002589, 2004.

Moysey, S., K. Singha and R. Knight, A framework for inferring field-scale rock physics relationships through numerical simulation, *Geophysical Research Letters,* 32: L08304, doi:10.1029/2004GL022152, 2005.

Mukerji, T., I. Takahashi and E. F. Gonzalez, Statistical rock physics: combining rock physics, information theory, and geostatistics to reduce uncertainty in seismic reservoir characterization, *The Leading Edge,* 20(3): 313–319, 2001.

Oldenburg, D. W. and Y. Li, Estimating the depth of investigation in dc resistivity and IP surveys, *Geophysics,* 64: 403–416, 1999.

Peck, A., S. Gorelick, G. d. Marsily, S. Foster and V. Kovalevsky, *Consequences of spatial variability in aquifer properties and data limitations for groundwater modelling practice*, Oxfordshire UK, IAHS Press, 272 p., 1988.

Purvance, D. T. and R. Andricevic, On the electrical-hydraulic conductivity correlation in aquifers, *Water Resources Research,* 36(10): 2905–2913, 2000.

Ramirez, A., W. Daily, D. LaBrecque, E. Owen and D. Chesnut, Monitoring an underground steam injection process using electrical resistance tomography, *Water Resources Research,* 29(1): 73–87, 1993.

Ramirez, A. L., J. J. Nitao, W. G. Hanley, R. Aines, R. E. Glaser, S. K. Sengupta, K. M. Dyer, T. L. Hickling and W. D. Daily, Stochastic inversion of electrical resistivity changes using a Markov Chain Monte Carlo approach, *Journal of Geophysical Research,* 110: B02101, doi:10.1029/2004JB003449, 2005.

Rector, J. W. and J. K. Washbourne, Characterization of resolution and uniqueness in crosswell direct-arrival traveltime tomography using the Fourier projection slice theorem, *Geophysics,* 59(11): 1642–1649, 1994.

Rubin, Y. and S. S. Hubbard, Eds., *Hydrogeophysics*, Springer, 2005.

Rubin, Y., G. Mavko and J. Harris, Mapping permeability in heterogeneous aquifers using hydrologic and seismic data, *Water Resources Research,* 28(7): 1809–1816, 1992.

Schuster, G. T., Resolution limits for crosswell migration and traveltime tomography, *Geophysical Journal International,* 127: 427–440, 1996.

Sheng, J. and G. T. Schuster, Finite-frequency resolution limits of wave path traveltime tomography for smoothly varying velocity models, *Geophysical Journal International,* 152(3): 669–676, 2003.

Singha, K. and S. M. Gorelick, Saline tracer visualized with electrical resistivity tomography: field scale moment analysis, *Water Resources Research,* 41: W05023, doi:10.1029/2004WR003460, 2005.

Singha, K. and S. M. Gorelick, Hydrogeophysical tracking of 3D tracer migration: the concept and application of apparent petrophysical relations, *Water Resources Research,* 42 W06422, doi:10.1029/2005WR004568, 2006.

Singha, K. and S. Moysey, Accounting for spatially variable resolution in electrical resistivity tomography through field-scale rock physics relations, *Geophysics,* 71(4): A25–A28, 2006.

Slater, L., A. Binley, R. Versteeg, G. Cassiani, R. Birken and S. Sandberg, A 3D ERT study of solute transport in a large experimental tank, *Journal of Applied Geophysics,* 49: 211–229, 2002.

Topp, G. C., J. L. Davis and A. P. Annan, Electromagnetic determination of soil water content: measurements in coaxial transmission lines, *Water Resources Research,* 16(3): 574–582, 1980.

Urish, D. W., Electrical resistivity-hydraulic conductivity relationships in glacial outwash aquifers, *Water Resources Research,* 17(5): 1401–1407, 1981.

Vanderborght, J., A. Kemna, H. Hardelauf and H. Vereecken, Potential of electrical resistivity tomography to infer aquifer transport characteristics from tracer studies: A synthetic case study, *Water Resources Research,* 41: W06013, doi:10.1029/2004WR003774, 23 pp., 2005.

VanMarcke, R., *Random Fields: Analysis and Synthesis*, Cambridge, MA, MIT Press, 1983.

Vereecken, H., A. Binley, G. Cassiani, A. Revil and K. Titov, Eds., *Applied Hydrogeophysics*, NATO Science Series: IV: Earth and Environmental Sciences, Springer-Verlag, 2006.

Wang, P. and R. Horne, N., *Integrating resistivity data with production data for improved reservoir modelling*, SPE Asia Pacific Conference of Integrated Modelling for Asset Management, Yokohama, Japan, Society of Petroleum Engineers, 2000.

Western, A. W., G. Bloschl and R. B. Grayson, How well do indicator variograms capture connectivity of soil moisture?, *Hydrological Processes,* 12: 1851–1868, 1998.

Yeh, T. C. J., S. Liu, R. J. Glass, K. Baker, J. R. Brainard, D. L. Alumbaugh and D. LaBrecque, A geostatistically based inverse model for electrical resistivity surveys and its applications to vadose zone hydrology, *Water Resources Research,* 38(12): 14-1:14-13, 2002.

Zinn, B. and C. F. Harvey, When good statistical models of aquifer heterogeneity go bad: a comparison of flow, dispersion, and mass transfer in connected and multivariate Gaussian hydraulic conductivity fields, *Water Resources Research,* 39(3): doi: 10.1029/2001WR001146, 2003.

F. D. Day-Lewis, U.S. Geological Survey, Office of Ground Water, Branch of Geophysics, 11 Sherman Place, Unit 5015, Storrs, CT 06269, USA. (daylewis@usgs.gov)

S. Moysey, School of the Environment, Clemson University, P.O. Box 340919, Clemson, SC 29634-0919, USA. (smoysey@clemson.edu)

K. Singha, Department of Geosciences, Pennsylvania State University, 311 Deike Building, University Park, PA 16802, USA. (ksingha@psu.edu)